Host–Guest Systems

DOI: 10.1002/ange.200501888

Escape from a Nonporous Solid: Mechanically Coupled Biconcave Molecules**

*Justin A. Riddle, John C. Bollinger, and Dongwhan Lee**

Molecular motions play a central role in many biologically important processes.[1] The correlated movement of a finite number of symmetrically disposed building blocks in naturally occurring constructs can amplify a local distortion into a global structural change.[2,3] This process is well illustrated by the unidirectional rotation of C_3-symmetric transmembrane protein complexes[4] and the pH-induced conformational changes of viral fusion proteins,[5] which continue to inspire synthetic mimics of their structural as well as functional properties.[6–9] Relaying mechanical signals to remote sites within such functional aggregates requires structurally rigid units, and the noncovalent interactions between these units can be maximized by positioning them in a symmetric fashion. In an effort to implement such an architectural motif in a small-molecule setting, we have devised a general synthetic

[*] J. A. Riddle, Dr. J. C. Bollinger, Prof. Dr. D. Lee
Department of Chemistry and Molecular Structure Center
Indiana University, Bloomington, IN 47405 (USA)
Fax: (+1) 812-855-8300
E-mail: dongwhan@indiana.edu

[**] This work was supported by Indiana University. We also acknowledge the donors of the American Chemical Society Petroleum Research Fund for their support of this research. J.A.R. gratefully acknowledges a GAANN Fellowship from the U.S. Department of Education.

Supporting information for this article, including the synthesis, characterization, and crystallographic data for compounds **4**–**6**, is available on the WWW under http://www.angewandte.org or from the author.

© 2005 Wiley-VCH Verlag GmbH & Co. KGaA, Weinheim

route to a new class of C_3-symmetric biconcave molecules. The solid-state structures of these molecules reveal effective mechanical communication between two vertices, by which structural changes on one side of the molecule are effectively transmitted to the other side (Scheme 1). Remarkably, the flexible solid-state structure of one such compound allows the complete release of clathrated guest molecules from a nonporous solid under ambient conditions. This dynamic crystal-to-crystal transformation has been confirmed by single-crystal X-ray crystallography.

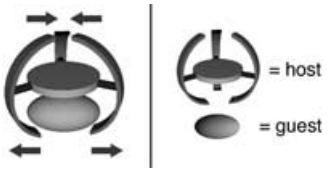

Scheme 1. Schematic representation of conformational transmission by correlated opening and closing of the two concave sides of a molecule.

We developed a convergent synthetic route in order to realize the mechanical coupling illustrated in Scheme 1. Our molecular design positions three *m*-terphenyl "wings" at the periphery of a C_3-symmetric core. The six wing-tips of these elongated aromatic groups converge to define the two vertices of a biconcave molecule. As each pseudo-C_2-symmetric terphenyl unit is disposed nearly perpendicular to the disc-shaped core, expansion of one cavity was expected to nicely correlate with contraction of the other (Scheme 1). Preliminary molecular modeling suggested that a triphenylene-type core **2** (Scheme 2) should be able to support three symmetrically disposed *m*-terphenyl fragments without severe steric constraints. As a structural surrogate of this planar polyaromatic platform, tris(salicylideneamine) **1**[10,11] (Scheme 2) was chosen in our synthesis. In addition to assisting the facile construction of three-dimensional structures from modularly accessible building blocks, the semirigid six-membered rings afforded by the resonance-assisted hydrogen bonds (RAHBs)[12] were expected to better accommodate the structural changes depicted in Scheme 1.

The reaction between 1,3,5-triformylphloroglucinol (**3**)[10] and five equivalents of 2,6-di(*p*-methoxyphenyl)aniline[13] in EtOH at reflux cleanly afforded the desired Schiff base product **4** in over 85% yield (Scheme 2). The ^{1}H and ^{1}H–^{1}H COSY NMR spectra of this compound in CD_2Cl_2 at 25°C display a doublet ($\delta = 12.43$ ppm, 3H, =CN*H*) coupled ($J = 13$ Hz) to another doublet ($\delta = 7.53$ ppm, 3H, =C*H*N).[14] Upon treatment with D_2O, the resonance at lower field completely disappears and the upper-field signal merges into a sharp singlet. This observation is consistent with the keto-enamine tautomer of the C_3-symmetric tris(salicylideneamine) core rather than the enol-imine.[10,11] The six methyl groups in **4** could be removed by treatment with BBr_3 at −78°C to furnish **5** in a yield of 70%. A more sterically hindered homologue **6** could be obtained (65% yield) by triple Schiff base condensation of **3** with 2,6-dimesitylaniline.[13]

This high-yielding and operationally simple route afforded **4–6** in four to five steps from readily available materials without the need for chromatographic separation of synthetic intermediates. Notably, the selective formation of C_3-symmetric **4–6** stands in stark contrast to the previous synthesis of less hindered tris(salicylideneamine) derivatives,[15] in which mixtures of C_s and C_3 isomers were generally obtained (Scheme 2).[10,11] By defining symmetric spaces above and below the molecular core, the *m*-terphenyl fragments apparently suppress the formation of the undesired C_s isomer. The reaction between **3** and 2-(4-hydroxyphenyl)aniline still furnished a mixture of C_s and C_3 isomers ($\approx$3:1 ratio).

The nine aromatic rings in each of **4–6** are all connected by single C–C bonds rather than by direct ring fusion, thus allowing a balance between structural rigidity and flexibility. As shown in Scheme 3,[16,17] the three *m*-terphenyl wings can undergo concerted tilting with respect to the threefold axis.[18] Intramolecular steric considerations demand that this molecular motion proceeds in a merry-go-round fashion to establish a pair of C_3-symmetric enantiomers, similar to the Δ and Λ isomers of an octahedral tris(chelate)–metal complex. The pseudo-Δ and pseudo-Λ enantiomers are present in equal amounts in solids **4–6**.

As part of this iris-like opening and closing motion, **5** displays conformational communication between two vertices in that the opening of one concave side closes the other side of the molecule (Figure 1).[19] The pronounced asymmetry of the cavity topology is reflected by the distances between adjacent *m*-terphenyl wing-tips on each side

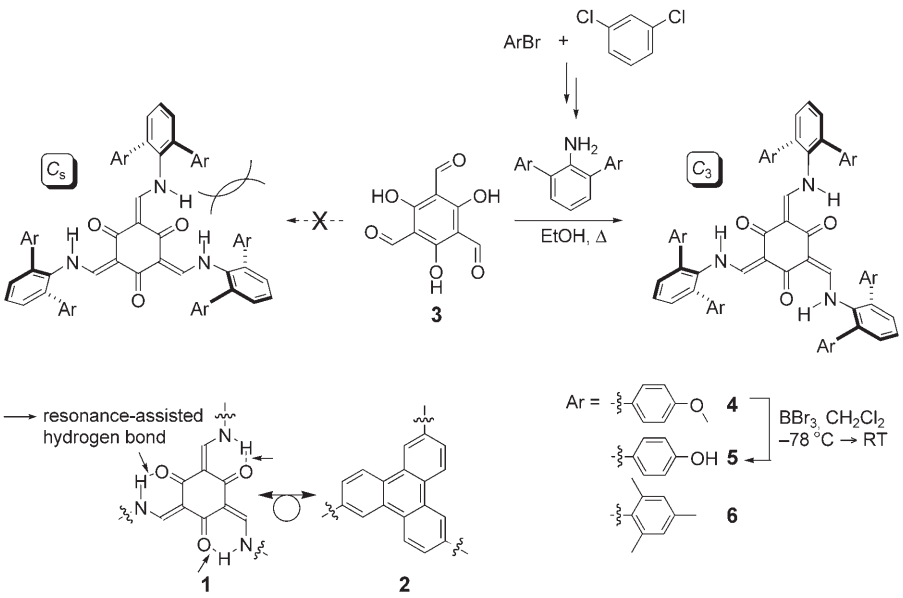

Scheme 2. Synthetic routes to C_3-symmetric biconcave hosts **4–6**.

© 2005 Wiley-VCH Verlag GmbH & Co. KGaA, Weinheim

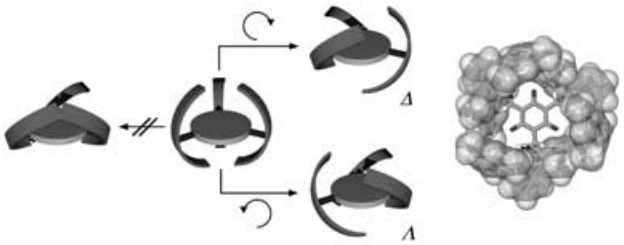

Scheme 3. Iris-like opening and closing motion: concerted tilting affords an enantiomeric pair of open conformers (right); reversing one rotation imposes steric constraints between adjacent *m*-terphenyl groups (left). Shown next to the schematic diagram is a capped-stick (core) and space-filling (mesityl groups) representation of the crystal structure of **6** (only the *Λ* isomer is shown).

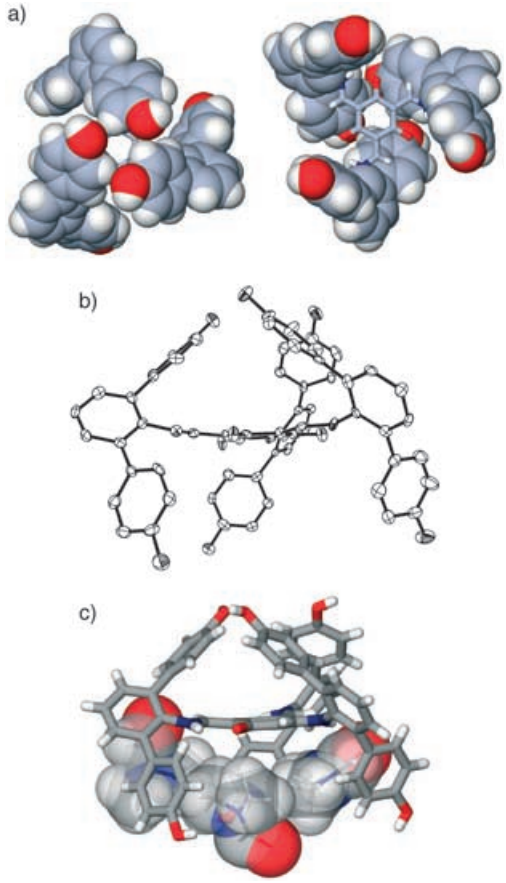

Figure 1. Crystal structure of **5**·6.5 DMF: a) space-filling and capped-stick representations viewed from the top (left) and bottom (right) of the molecule (DMF molecules are omitted); b) ORTEP diagram with thermal ellipsoids at the 50% probability level (hydrogen atoms and DMF guests have been omitted for clarity); c) three DMF molecules (in space-filling model) occupy the open concave side of **5** (capped-stick representation).

of the molecule: the "open" side $C_{para}\cdots C_{para}$ distances range from 10.470 to 10.988 Å (mean value: 10.697 Å), whereas the "closed" side distances range from 5.183 to 5.491 Å (mean value: 5.339 Å). In the solid state, three molecules of DMF (*N*,*N*-dimethylformamide) are located on one concave side of **5**. Although the detailed nature of this van der Waals host–guest interaction is yet to be elucidated, this adaptive structural change convincingly demonstrates the conformational transmission proposed in Scheme 1.

The immediate functional relevance of structural semirigidity was highlighted by a single-crystal-to-single-crystal transformation of **4**, in which clathrated $CHCl_3$ molecules completely escape the crystal lattice without disrupting it. Compound **4** crystallizes in the trigonal system (space group *P*31*c*). Two chemically identical, but crystallographically unique, molecules **4a** and **4b** were identified in the lattice, each having a crystallographic threefold axis passing through the molecular core (Figure 2a). In the solid state, facing pairs

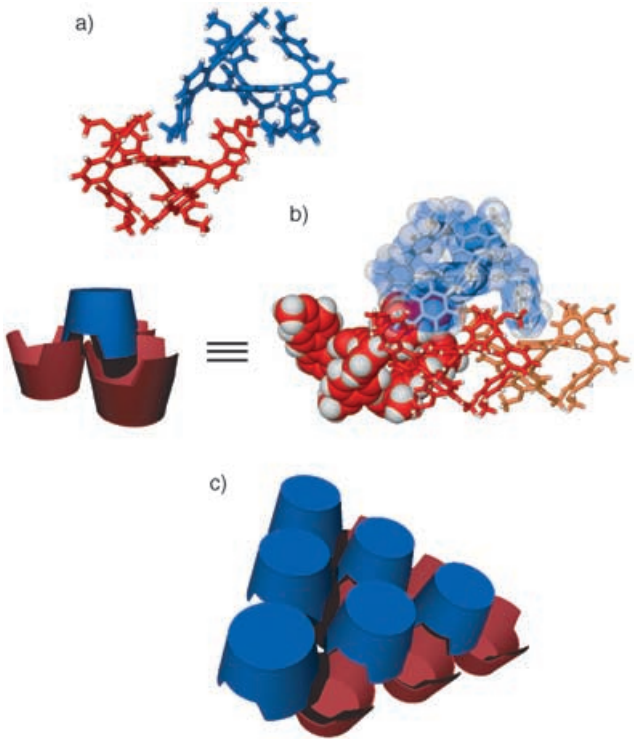

Figure 2. Molecular packing of **4a** (blue) and **4b** (red) in solvent-free solid **4**: a) capped-stick representation of two unique molecules interpenetrating each other; b) interaction between **4a** and a trigonal array of **4b**; c) schematic representation of a portion of the interdigitated bilayer comprising **4a** (six molecules, top) and **4b** (six molecules, bottom).

of **4a** and **4b** interpenetrate each other to open one side of the molecule and close up the other side. The *m*-terphenyl wings on the open side of **4a** function as a tripod when it docks with a triangular array of molecules of **4b** underneath (Figure 2b). In turn, each molecule of **4b** is associated with three **4a** molecules stacked on top of it, thus defining repeating interdigitated bilayers of **4a**·**4b** perpendicular to the crystallographic *c* axis (Figure 2c). The overall shape complementarity of the C_3-symmetric **4** reinforces intermolecular van der Waals contacts and assists in efficient molecular packing. As a result, only 3.9% of the crystal volume is available to guests.

Evenly spaced interstitial spaces were identified within the two-dimensional closest packed layer of **4** (Figure 3). Each of these C_3-symmetric crevices, with a volume of around

 © 2005 Wiley-VCH Verlag GmbH & Co. KGaA, Weinheim

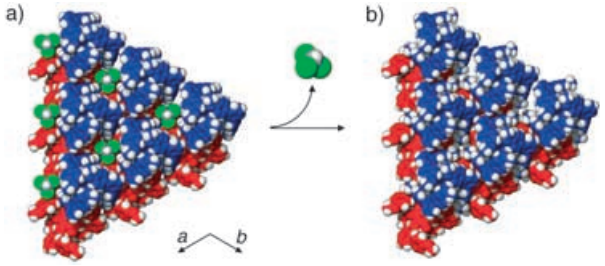

Figure 3. a) Crystal structure of a portion of **4**·1/2 $CHCl_3$, shown as a space-filling representation of six **4a** molecules (blue) stacked on top of six **4b** molecules (red) viewed along the crystallographic *c* axis. Every interstitial void space is surrounded by a triangular array of **4a** and fully occupied by one molecule of $CHCl_3$ (green), which is disordered over two positions (not illustrated). b) Crystal structure of **4** redetermined after the complete release of $CHCl_3$.

112 $Å^3$, is centered over a triangular array of **4a** and is fully occupied by one molecule of $CHCl_3$ when **4** is recrystallized from $CHCl_3/Et_2O$.[20] After standing at room temperature for 10 weeks, the co-crystal of **4** and $CHCl_3$ perfectly retained its crystallinity despite the complete loss of $CHCl_3$ from the interstitial space. This was confirmed by a redetermination of the X-ray crystal structure of the same crystal, which also revealed a substantial ($\approx$4.3%) decrease in the volume of the unit cell.[21,22] Except for C_{aryl}–C_{aryl} rotations involving three *p*-methoxylphenyl groups of **4a** close to $CHCl_3$ (Figure 4), no significant structural changes were observed before and after solvent loss. The rigid tris(salicylideneamine) cores perfectly fit each other with a maximum deviation of less than 0.05 Å, and the aryl groups on the closed side of **4a** show a maximum deviation of 0.270 Å. The structure of **4b** revealed deviations of less than 0.250 Å for all atoms.[14]

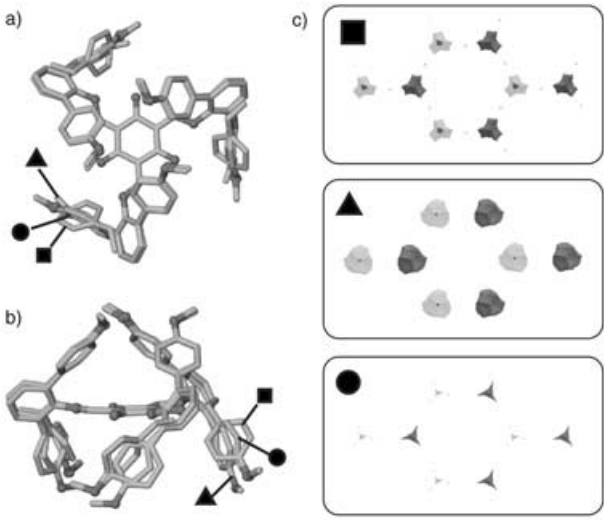

Figure 4. a) Overlaid structures of **4a** in capped-stick representations viewed along the crystallographic threefold axis. b) Perpendicular view. For each conformer, all three *m*-terphenyl groups are related by crystallographic C_3 symmetry. Structures ■ and ▲, which are related by positional disorder of 0.13 and 0.87 site occupancy, respectively, were obtained before the release of $CHCl_3$, whereas ● is from the desolvated crystal. c) Cavities in the crystal structures of **4** corresponding to different conformations ■, ▲, and ● viewed along the crystallographic *c* axis. The surface of the cavities was constructed by tracing the center of a van der Waals sphere of 4.5 Å diameter as it rolls over the surface of **4** within a 2×2×1 array of unit cells. Dark gray surfaces correspond to voids in the upper layer and light gray surfaces correspond to those in the lower layer when viewed along the crystallographic *c* axis. The van der Waals volume of $CHCl_3$, calculated to be about 75 $Å^3$, corresponds to that of a spherical object with a diameter of about 5 Å. Therefore, the actual space explored by the center of $CHCl_3$ should reside within the cavity surfaces depicted in this figure.

Unlike conventional microporous materials developed for the uptake and release of small-molecule substrates,[23] no unobstructed channels could be found that connect individual cavities within **4** (Figure 4).[24] Escape of $CHCl_3$ therefore requires a cooperative movement within the crystal lattice, which could provide a transient passage for $CHCl_3$ in its hopping between adjacent interstitial voids.[25,26] We suggest that C_{aryl}–C_{aryl} rotations of **4a** accompany this process because its overlaid X-ray crystal structures reveal a concerted movement of three *m*-terphenyl groups in response to the departure of adjacent $CHCl_3$ molecules.[14] As shown in Figure 4, the contours of the accessible surface also exhibit drastic morphological changes following this motion.

We note that structural distortions might seem insignificant at the single-molecule level, but their collective effects could be amplified by interlocking arrangements within higher-order assemblies (Figure 2). Harnessing the flexibility of a loosely held aromatic-rich scaffold could be a viable approach to amplifying adaptive molecular motions. This is currently being investigated in our laboratory.

Received: May 31, 2005
Revised: June 26, 2005
Published online: September 19, 2005

Keywords: crystal engineering · host–guest systems · receptors · self-assembly · supramolecular chemistry

[1] M. Schliwa, *Molecular Motors*, Wiley-VCH, Weinheim, **2003**.
[2] D. S. Goodsell, A. J. Olson, *Annu. Rev. Biophys. Biomol. Struct.* **2000**, *29*, 105–153.
[3] G. Krauss, *Biochemistry of Signal Transduction and Regulation*, 3rd ed., Wiley-VCH, Weinheim, **2003**.
[4] a) V. Koronakis, A. Sharff, E. Koronakis, B. Luisi, C. Hughes, *Nature* **2000**, *405*, 914–919; b) C. Andersen, E. Koronakis, E. Bokma, J. Eswaran, D. Humphreys, C. Hughes, V. Koronakis, *Proc. Natl. Acad. Sci. USA* **2002**, *99*, 11103–11108; c) V. Koronakis, *FEBS Lett.* **2003**, *555*, 66–71.
[5] J. J. Skehel, D. C. Wiley, *Cell* **1998**, *95*, 871–874.
[6] V. Balzani, A. Credi, F. M. Raymo, J. F. Stoddart, *Angew. Chem.* **2000**, *112*, 3484–3530; *Angew. Chem. Int. Ed.* **2000**, *39*, 3348–3391.
[7] V. Balzani, M. Venturi, A. Credi, *Molecular Devices and Machines: A Journey into the Nanoworld*, Wiley-VCH, Weinheim, **2003**.
[8] R. Krauss, U. Koert, *Synlett* **2003**, 598–608.
[9] J. Clayden, A. Lund, L. Vallverdú, M. Helliwell, *Nature* **2004**, *431*, 966–971.
[10] J. H. Chong, M. Sauer, B. O. Patrick, M. J. MacLachlan, *Org. Lett.* **2003**, *5*, 3823–3826.
[11] C. V. Yelamaggad, A. S. Achalkumar, D. S. S. Rao, S. K. Prasad, *J. Am. Chem. Soc.* **2004**, *126*, 6506–6507.

 © 2005 Wiley-VCH Verlag GmbH & Co. KGaA, Weinheim

[12] P. Gilli, V. Bertolasi, V. Ferretti, G. Gilli, *J. Am. Chem. Soc.* **2000**, *122*, 10405 – 10417.

[13] a) S. Sasaki, H. Hatsushiba, M. Yoshifuji, *Chem. Commun.* **1998**, 2221 – 2222; b) B. Twamley, C.-S. Hwang, N. J. Hardman, P. P. Power, *J. Organomet. Chem.* **2000**, *609*, 152 – 160; c) J. Gavenonis, T. D. Tilley, *J. Am. Chem. Soc.* **2002**, *124*, 8536 – 8537.

[14] See Supporting Information.

[15] The only crystallographically characterized analogue of **4**–**6** is the condensation product of **3** and *N*-(*tert*-butyloxycarbonyl)-1,2-diaminobenzene.[10] The ^{1}H NMR spectrum of this compound, however, indicates the presence of both C_s and C_3 isomers.

[16] CCDC 273250 (**4**), 273251 (**4**·0.5 $CHCl_3$), 273252 (**5**·6.5 DMF), and 273253 (**6**·C_5H_{12}) contain the supplementary crystallographic data for this paper. These data can be obtained free of charge from the Cambridge Crystallographic Data Centre via www.ccdc.cam.ac.uk/data_request/cif.

[17] Crystallographic data for **6**·C_5H_{12}: $0.35\times0.30\times0.10\ mm^3$, triclinic, space group $P\bar{1}$, $a=15.3889(12)$, $b=16.0641(12)$, $c=16.8427(13)$ Å, $\alpha=98.072(2)°$, $\beta=93.593(2)°$, $\gamma=118.488(2)°$, $V=3582.8(5)$ Å^3, and $\rho_{calcd}=1.128\ g\,cm^{-3}$ at 125 K. Data were collected by ω scans with $Mo_{K\alpha}$ radiation ($\lambda=0.71073$ Å), and all available reflections to $2\theta_{max}=50°$ were harvested (65417 reflections, 12610 unique) and corrected for Lorentz and polarization factors with Bruker SAINT 6.45 A. Reflections were subsequently corrected for absorption (empirical correction, $\mu=0.067\ mm^{-1}$), interframe scaling, and other systematic errors with SADABS 2004/1 (combined transmission and other correction factors min./max. = 0.977/0.993). The structure was solved (direct methods) and refined (full-matrix least-squares against F^2) with the Bruker SHELXTL package (version 6.12). All reflections were used in the refinement of 901 parameters, in which hydrogen atoms were refined with a riding model (R_F(observed data) = 0.0585, R_F^2(all data) = 0.1818, maximum residual density = 0.539 e$^-$ Å^{-3}).

[18] For correlated rotations in *n*-fold molecular rotors, see: a) S. Brydges, L. E. Harrington, M. J. McGlinchey, *Coord. Chem. Rev.* **2002**, *233–234*, 75 – 105; b) G. S. Kottas, L. I. Clarke, D. Horinek, J. Michl, *Chem. Rev.* **2005**, *105*, 1281 – 1376, and references therein.

[19] Crystallographic data for **5**·6.5 DMF: Twinned crystal of $0.28\times0.22\times0.12\ mm^3$, triclinic, space group $P\bar{1}$, $a=15.760(5)$, $b=16.863(5)$, $c=16.878(5)$ Å, $\alpha=60.127(11)°$, $\beta=82.659(11)°$, $\gamma=84.258(10)°$, $V=3854.1(19)$ Å^3, and $\rho_{calcd}=1.260\ g\,cm^{-3}$ at 122 K. Data were collected by ω scans with $Mo_{K\alpha}$ radiation ($\lambda=0.71073$ Å), and all available reflections to $2\theta_{max}=50°$ were harvested (50955 reflections, 20663 unique, including unique combinations of twin component contributions) and corrected for Lorentz and polarization factors with Bruker SAINT 6.45A. Reflections were subsequently corrected for absorption (empirical correction, $\mu=0.088\ mm^{-1}$), interframe scaling, and other systematic errors with TWINABS 1.05 (combined transmission and other correction factors min./max. = 0.781/0.989). The structure was solved (direct methods) and refined (full-matrix least-squares against F^2) with the Bruker SHELXTL package (version 6.12). All reflections were used in the refinement of 1059 parameters, in which hydrogen atoms were refined with a riding model. (R_F(observed data) = 0.0778, R_F^2(all data) = 0.1930, maximum residual density = 0.480 e$^-$ Å^{-3}).

[20] Crystallographic data for **4**·0.5 $CHCl_3$: $0.31\times0.30\times0.15\ mm^3$, trigonal, space group $P31c$, $a=16.9447(14)$, $c=24.072(4)$ Å, $V=5985.7(12)$ Å^3, and $\rho_{calcd}=1.256\ g\,cm^{-3}$ at 123 K. Data were collected by ω scans with $Mo_{K\alpha}$ radiation ($\lambda=0.71073$ Å), and all available reflections to $2\theta_{max}=50°$ were harvested (104520 reflections, 7053 unique) and corrected for Lorentz and polarization factors with Bruker SAINT 6.45A. Reflections were subsequently corrected for absorption (empirical correction, $\mu=0.082\ mm^{-1}$), interframe scaling, and other systematic errors with SADABS 2004/1 (combined transmission and other correction factors min./max. = 0.814/0.983). The structure was solved (direct methods) and refined (full-matrix least-squares against F^2) with the Bruker SHELXTL package (version 6.12). All reflections were used in the refinement of 703 parameters, including full isotropic refinement of most hydrogen atoms but riding refinement for low-occupancy hydrogen atoms of one disordered group (R_F(observed data) = 0.0404, R_F^2(all data) = 0.1100, maximum residual density = 0.276 e$^-$ Å^{-3}).

[21] Crystallographic data for **4**: $0.31\times0.30\times0.15\ mm^3$, trigonal, space group $P31c$, $a=16.7934(14)$, $c=23.463(2)$ Å, $V=5730.5(7)$ Å^3, and $\rho_{calcd}=1.243\ g\,cm^{-3}$ at 121 K. Data were collected by ω scans with $Mo_{K\alpha}$ radiation ($\lambda=0.71073$ Å), and all available reflections to $2\theta_{max}=50°$ were harvested (100574 reflections, 6742 unique) and corrected for Lorentz and polarization factors with Bruker SAINT 6.45A. Reflections were subsequently corrected for absorption (face-indexed correction, $\mu=0.082\ mm^{-1}$, transmission min./max. = 0.978/0.991, Bruker XPREP 2005/1) and for interframe scaling and other systematic errors (SADABS 2004/1). The structure was solved (direct methods) and refined (full-matrix least-squares against F^2) with the Bruker SHELXTL package (version 6.12). All reflections were used in the refinement of 639 parameters, including full isotropic refinement of all hydrogen atoms (R_F(observed data) = 0.0338, R_F^2(all data) = 0.0868, maximum residual density = 0.369 e$^-$ Å^{-3}).

[22] Diffraction data for a precise structural comparison were collected for the same crystal at essentially the same temperatures. See references [20] and [21].

[23] For recent reviews, see: a) M. Eddaoudi, D. B. Moler, H. Li, B. Chen, T. M. Reineke, M. O'Keeffe, O. M. Yaghi, *Acc. Chem. Res.* **2001**, *34*, 319 – 330; b) B. Moulton, M. J. Zaworotko, *Chem. Rev.* **2001**, *101*, 1629 – 1658; c) O. M. Yaghi, M. O'Keeffe, N. W. Ockwig, H. K. Chae, M. Eddaoudi, J. Kim, *Nature* **2003**, *423*, 705 – 714; d) S. Kitagawa, R. Kitaura, S.-i. Noro, *Angew. Chem.* **2004**, *116*, 2388 – 2430; *Angew. Chem. Int. Ed.* **2004**, *43*, 2334 – 2375; e) *Acc. Chem. Res.* **2005**, *38*, 215 – 378 (special issue on molecular architecture).

[24] For recent demonstrations of the uptake and release of small molecules by nonporous molecular structures, see: a) J. L. Atwood, L. J. Barbour, A. Jerga, *Science* **2002**, *296*, 2367 – 2369; b) G. D. Enright, K. A. Udachin, I. L. Moudrakovski, J. A. Ripmeester, *J. Am. Chem. Soc.* **2003**, *125*, 9896 – 9897; c) J. L. Atwood, L. J. Barbour, A. Jerga, *Angew. Chem.* **2004**, *116*, 3008 – 3010; *Angew. Chem. Int. Ed.* **2004**, *43*, 2948 – 2950; d) P. K. Thallapally, G. O. Lloyd, J. L. Atwood, L, J. Barbour, *Angew. Chem.* **2005**, *117*, 3916 – 3919; *Angew. Chem. Int. Ed.* **2005**, *44*, 3848 – 3851.

[25] The rotation of *tert*-butyl groups has been proposed to assist release of entrapped gaseous molecules from a nonporous solid matrix of *p-tert*-butylcalix[4]arene: J. L. Atwood, L. J. Barbour, P. K. Thallapally, T. B. Wirsig, *Chem. Commun.* **2005**, 51 – 53.

[26] For a highly synchronized phase transition that assists the transport of guest molecules in the absence of continuous channels, see: J. L. Atwood, L. J. Barbour, A. Jerga, B. L. Schottel, *Science* **2002**, *298*, 1000 – 1002.

 © 2005 Wiley-VCH Verlag GmbH & Co. KGaA, Weinheim